Article:
Chu, F, Wen, D and Wu, X (2018) Frost Self-Removal Mechanism during Defrosting on Vertical Superhydrophobic Surfaces: Peeling Off or Jumping Off. Langmuir, 34 (48). pp. 14562-14569. ISSN: 0743-7463

https://doi.org/10.1021/acs.langmuir.8b03347

Frost self-removal mechanism during defrosting on vertical superhydrophobic surfaces: peel off or jump off

Fuqiang Chu [a,b], Dongsheng Wen [a], Xiaomin Wu *, [b]

[a] School of Aeronautic Science and Engineering, Beihang University, Beijing, China

[b] Key Laboratory for Thermal Science and Power Engineering of Ministry of Education, Beijing Key Laboratory for CO_2 Utilization and Reduction Technology, Department of Energy and Power Engineering, Tsinghua University, Beijing, China

Abstract

Although a superhydrophobic surface has potentials to delay frosting, it fails finally when conditions are too harsh, so defrosting is still essential. Here, we investigated the frost self-removal mechanism during defrosting on vertical superhydrophobic surfaces. Owing to the great water repellency of the superhydrophobic surface and the water absorption of porous frost, meltwater close to the surface tends to permeate into the frost layer. As frost density is much less than water density, the frost volume shrinks during defrosting. When the frost quantity is large, the permeation effect dominates because there is much porous frost. The permeation effect separates the unmelted frost layer from the superhydrophobic surface, as a result, the frost peels off by gravity completely. When the frost quantity is little, the permeation effect is negligible, while the volume shrinkage effect works, making the thin frost layer break up into many small pieces. These small frost pieces keep irregular shapes and continue to shrink, releasing large amounts of surface energy to drive themselves jump off from the superhydrophobic surface. However, compared with the peeling off mode, the jumping off mode is not so effective that there are still small droplets adhering on the surface after defrosting. This work may provide guides for defrosting application of superhydrophobic surfaces in related engineering fields.

1. Indroduction

Frosting formation exists widely in engineering fields such as aerospace, refrigeration and power generation, and causes numerous problems. The frost on an aircraft wing changes its aerodynamic configuration, reduces the wing lift and even imperils the flight safety;[1] the frost on heat exchanger fins blocks the flow channel, increases the thermal resistance and deteriorates the heat transfer;[2] the frost also changes the aerodynamic characteristics of a wind turbine and reduces its power generation efficiency.[3] Over the past decade, many efforts have been made to restrain the frost formation and the utilization of superhydrophobic surface with a contact angle more than 150^o and a contact angle hysteresis less than 10^o is indeed a good idea.[4-8] Researchers have demonstrated that the superhydrophobic surface has great advantages in delaying ice nucleation, reducing frost adhesion and even self-cleaning subcooled droplets by a spontaneous jumping motion.[9-15] However, although the superhydrophobic surface delays frosting to some extent, it would fail when exposed conditions are too harsh.[12-14, 16] Thus, periodic defrosting for frosted superhydrophobic surface is still essential.

Owing to its unique wettability, the superhydrophobic surface shows distinct defrosting characteristics. On horizontal superhydrophobic surfaces, the frost meltwater films first dewet by edge curling and then by shrinking or coalescence, and finally dewet into isolated droplets.[17] These droplets, which keep highly mobile Cassie state, are able to roll down at very small titled angles.[18-19] Like that occurred during condensation,[20-21] self-propelled jumping, rotating and sliding movements during defrosting also take place frequently, making the defrosting process very dynamic and generating very low surface coverages on superhydrophobic surfaces.[22-24] On vertical superhydrophobic surfaces, the defrosting process is more efficient that the melting frost departs from the

superhydrophobic surface directly at the early stage of defrosting.[25-27] Compared with conventional surfaces such as bare Aluminum surfaces and hydrophobic surfaces, the retention water mass or fraction presents a much lower value.[28-30] However, there are still questions unclear for the defrosting on superhydrophobic surface. For example, how does the frost depart from a vertical superhydrophobic surface during defrosting, slide down, peel off or jump off? What are the mechanisms and key influencing factors? In this work, we prepared Al-based superhydrophobic surfaces and conducted defrosting experiments on them, and try to determine the frost departure mechanism during defrosting on vertical superhydrophobic surfaces. We hope this work could push the applications of the superhydrophobic surface and provide guide for real defrosting operation in related engineering fields such as aircrafts, heat exchangers and wind turbines.

2. Experimental section

The experimental surfaces are Al-based superhydrophobic surfaces fabricated by the chemical etching-deposition method.[31] The surface structures observed by a scanning electron microscopy are shown in Fig. 1. As seen, there are hierarchical micro-nano structures on the superhydrophobic surface with the micro structures being aggregations of irregular nanoscale grains.[31] With these hierarchical structures, the surface maintains excellent superhydrophobicity. At room temperature (25°C), the static contact angle of a 2 μl droplet on the superhydrophobic surface is measured to be 160.0±0.5°, the measured advancing and receding contact angles by the titled plate method are 162.2±1.0° and 158.3±1.0°, respectively, as shown in Fig. 1.

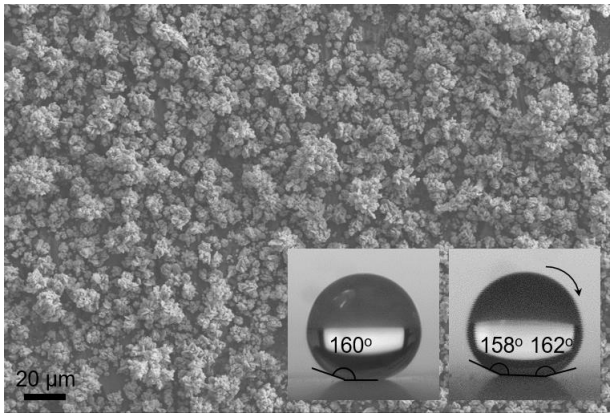

Figure 1. SEM images of the experimental superhydrophobic surface: hierarchical micro-nano structures evenly distribute on the superhydrophobic surface with the micro structure being aggregations of irregular nanoscale grains. The static, advancing and receding contact angles of the superhydrophobic surface are about 160°, 162° and 158°, respectively.

The experimental system and apparatus for frosting used here were same as those in our previous work.[32] The superhydrophobic surfaces were vertically placed on the cold side of a thermoelectric cooler, and the experiments were performed in a closed laboratory. Before defrosting experiments, frosting experiments are needed to accumulate moderate frost. During the frosting experiments, the laboratory temperature was measured to be 18.0±1.0°C with a relative air humidity of 90.0±5.0%, the cold surface temperature was −16.0±0.5°C. The frosting duration time was 10~30 min. After the frosting experiments, the power of the thermoelectric cooler was shut off and the heat was instantly transferred from the hot side of the thermoelectric cooler to the experimental surface and then to the frost. When the frost temperature rose above 0°C [33], the frost began to melt.[17]

3. Results and Discussion

3.1 Frost peel off during defrosting when frost quantity is large

Figure 2(a) shows the defrosting process on vertical superhydrophobic surface when the frosting duration is

20 min (See supporting information video S1). As the melting goes on, the frost first shrinks with cracks appearing on the frost layer (0~16.80 s), but the frost layer does not break up. Then, the upper edge of the frost layer separates from the surface (16.80~17.60 s) and the whole frost layer peels off from the surface by gravity completely (17.60~21.80 s). When the frost departs from the surface, it still keeps unmelted states. The frost peel off mechanism is explained in Fig. 2(b). Because of the much higher thermal conductivity of the Al-based surface than air, the heat flux transports from the hot side of the thermoelectric cooler to the surface and then to the frost more quickly, so the frost close to the surface first melts,[17] forming a water layer between the surface and the unmelted frost layer. Repulsed by the superhydrophobic surface with great water repellency and attracted by porous frost, the meltwater permeates into the frost layer quickly. Thus, the unmelted frost separates from the surface and peels off by gravity. Actually, when the frosting duration is long and the frost quantity is large, the meltwater permeation effect into the unmelted frost layer always dominates, separating the unmelted frost and the surface. Thus, the frost is removed by gravity as a way of peeling off. In the experiments that the frosting duration is 30 min, the peel off of frost from the superhydrophobic surface is more obvious (See supporting information video S2). The experiments by Kim et al. with large frost quantity also supports our conclusions.[30]

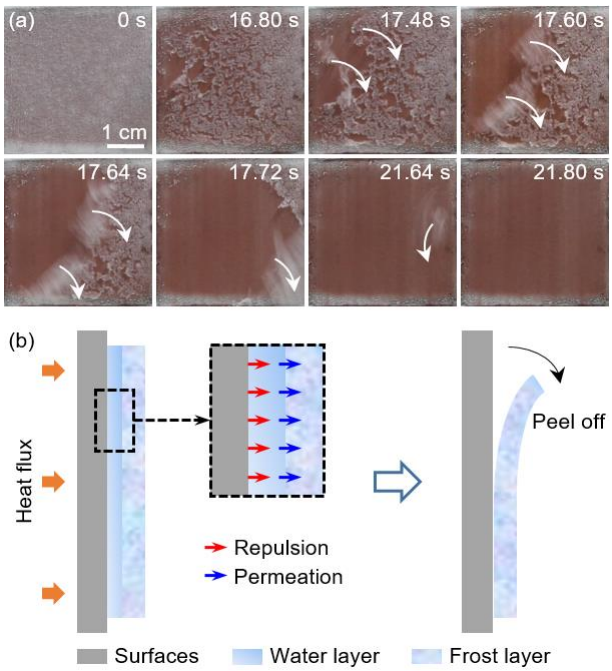

Figure 2. Peeling off of frost during defrosting on vertical superhydrophobic surfaces. (a) Experiments: the upper edge of the frost layer separates from the surface and the whole frost layer peels off from the surface by gravity (See supporting information video S1); (b) mechanisms: the meltwater in the water layer permeates into the unmelted frost layer, separating the unmelted frost and the surface, then the unmelted frost peels off by gravity.

3.2 Frost jump off during defrosting when frost quantity is little

When the frosting duration is 10 min with relatively less frost accumulated, the defrosting process on a vertical superhydrophobic surface is quite different, as shown in Fig. 3(a) (See supporting information video S3). Because the frost quantity is less, the volume shrinkage effect during frost melting plays a key role, it makes the frost break up into many small pieces with millimeter scale. As reported in literature which contains our own work, large amounts of surface energy can be released during the shrinking of melting frost with irregular shape, which easily triggers a self-propelled movement such as jumping.[22-24] As seen in Fig.3(a), the self-propelled jumping of melting frost indeed occurs very frequently (the solid circles represent original frost, the dashed circles show clean surfaces after jumping, and the white arrows indicate shadows of jumping paths). These jumping movements are able to self-remove most frost pieces, leaving an almost clean surface. Figure 3(b) are schematic diagram of the self-removal

process during defrosting on vertical superhydrophobic surfaces when the frost quantity is little. The volume shrinkage effect during melting make the frost layer break up into small pieces of frost, which then jump off from the surface.

However, although most frost pieces jump off from the superhydrophobic surface, there are still some small droplets adhering on the surface, as shown in the image at 21 s in Fig. 3(a). This is because that the jumping is an energy controlled phenomenon during which various energy including surface energy, viscous dissipation, work of adhesion, work of the retentive force and kinetic energy involved.[34-36] Only when the released surface energy is enough to overcome the viscous dissipation and other negative energy, the jumping would be triggered. The value of these energy forms are related to the size, the shape and the wetting mode of the melting frost, as well as the surface wettability. That means, not every piece of melting frost could jump off the surface, those who did not jump would melt into droplets and adhere on the surface.

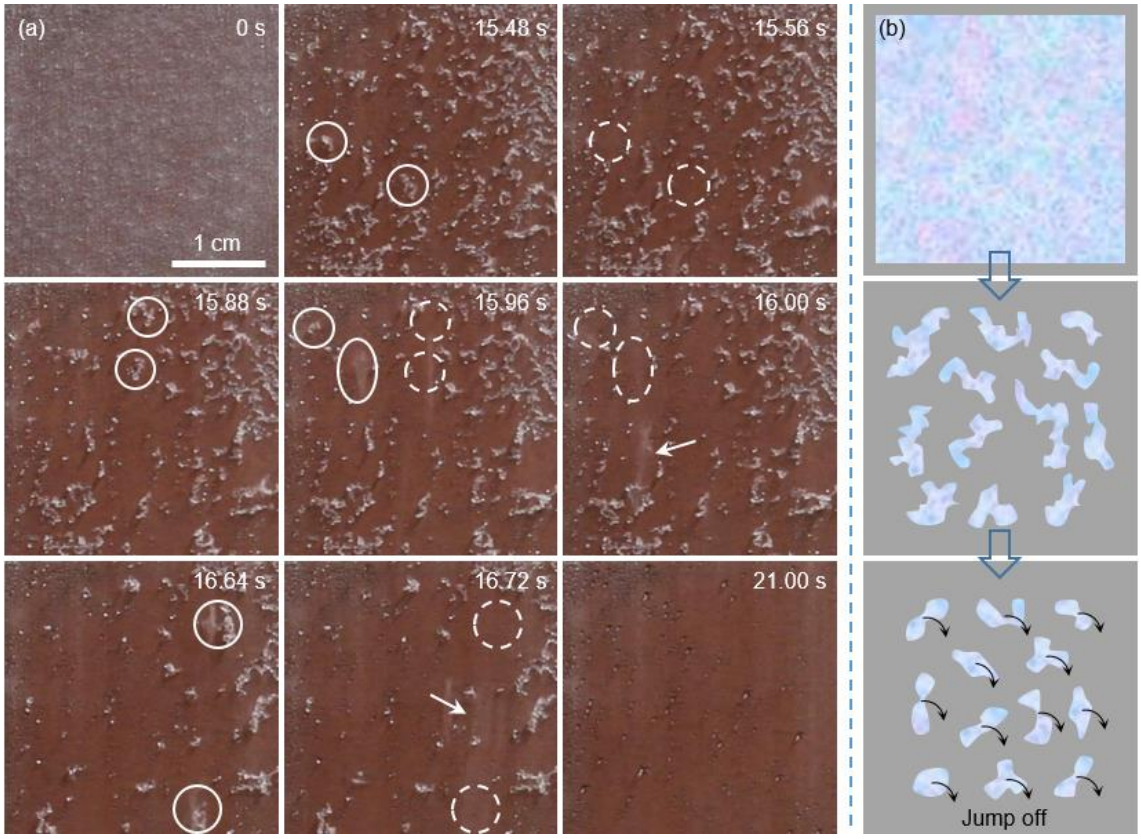

Figure 3. (a) Experiments (See supporting information video S3) and (b) schematic diagram of the jumping off process of frost during defrosting on vertical superhydrophobic surfaces. The volume shrinkage effect during melting make the frost layer break up into small pieces of frost, which then continue to shrink, releasing large amounts of surface energy to trigger the melting frost to jump off from the surface.

For the image at 21 s in Fig. 3(a), using proper image processing method,[32] we extracted the profile of residual droplets and measured every droplet's radius. Figure 4 shows the profiles and statistical results of residual droplets. A total of 110 droplets were counted with their radii within the range from 0.15 to 0.45 mm. More than 76% of residual droplets locate in the radius range of 0.2~0.3 mm, only 7% of residual droplets whose radii are more than 0.35 mm. The average radius (r_{ave}) was calculated to be 0.25 mm with a standard deviation of 0.06 mm.

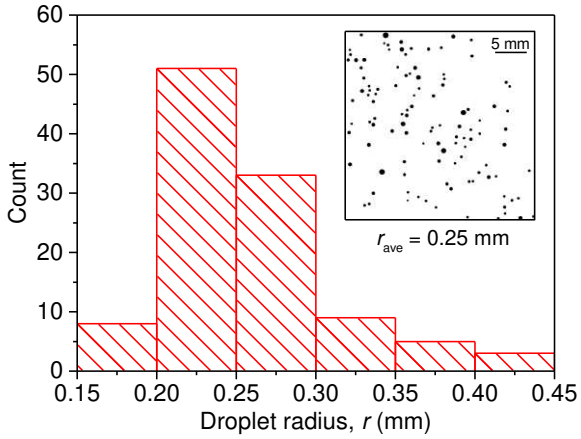

Figure 4. Profiles and statistical results of residual droplets on vertical superhydrophobic surface after defrosting when the frosting duration is 10 min. The radii range is from 0.15 to 0.45 mm with an average radius (r_{ave}) being about 0.25 mm. Most residual droplets (more than 76%) locate in the radius range of 0.2~0.3 mm.

For a meltwater droplet adhering on a vertical surface, two forces are balanced including the gravity and the retentive force, as shown in Fig. 5. The gravity of the droplet is given by

$$G = \rho g V \tag{1}$$

where ρ is the water density; g is the gravitational acceleration; V is the droplet volume, given by

$$V = \frac{2 - 3\cos\theta_0 + \cos^3\theta_0}{3}\pi r^3 \tag{2}$$

where r is the droplet radius; θ_0 is the surface static contact angle.

The accessible maximum retentive force due to the contact angle hysteresis is calculated as [37-39]

$$F_{cah} = kw\gamma_{lg}\left(\cos\theta_r - \cos\theta_a\right) \tag{3}$$

where γ_{lg} is the liquid-gas surface tension; θ_a and θ_r are the advancing and receding contact angles; k is a corrected coefficient; w is the maximum droplet contact width. For a droplet on a vertical surface, the real contact angle along the triple phase contact line varies with the azimuthal angle, φ.[40] When φ=0°, θ=θ_a; φ=180°, θ=θ_r; φ=90°, θ=θ_0. Thus, the maximum droplet contact width, which corresponds to φ=90°, can be estimated as

$$w = 2r\sin\theta_0 \tag{4}$$

Considering that the gravity and the accessible maximum retentive force are balanced, a critical droplet radius can be obtained as

$$r_{cri} = \left[\frac{6k\gamma_{lg}\left(\cos\theta_r - \cos\theta_a\right)\sin\theta_0}{\pi\left(2 - 3\cos\theta_0 + \cos^3\theta_0\right)\rho g}\right]^{\frac{1}{2}} \tag{5}$$

When the real radius of a droplet is more than the critical value, gravity dominates, the droplet rolls down from the surface; otherwise, the retentive force dominates, the droplet adheres on the surface.

For the Al-based superhydrophobic surface used here, the static, advancing and receding contact angles of the superhydrophobic surface are measured to be 160.0±0.5°, 162.2±1.0° and 158.3±1.0°. According to Eq. (5), with k set to be 2,[17] the calculated critical radius is 0.23±0.06 mm, which is quite consistent with the statistical average droplet radius (0.25±0.06 mm) with a relative deviation of 8%.

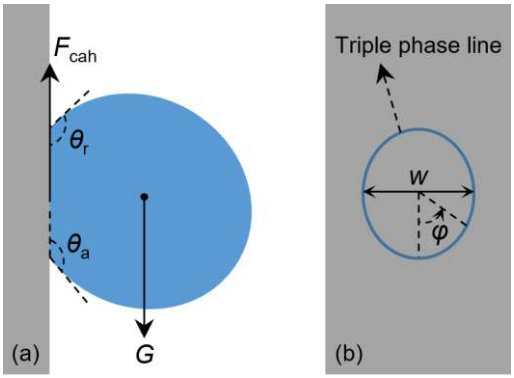

Figure 5. (a) Force analysis of a droplet adhering on vertical surfaces. G is gravity of the droplet, F_{cah} is the retentive force due to the surface contact angle hysteresis. (b) The triple phase contact line of the adhering droplet. w is the maximum droplet contact width, φ is the azimuthal angle along the triple phase line.

4. Conclusions

We conducted defrosting experiments on vertical Al-based superhydrophobic surfaces and investigated the frost self-removal modes. When the frosting duration is long and the frost quantity is large, the frost departs from the superhydrophobic surface by a way of peeling off. During defrosting for large frost quantity, the permeation effect plays a key effect that the meltwater close to the superhydrophobic surface permeates into the unmelted frost layer, separating the frost layer and the surface, so the frost layer peels off from the superhydrophobic surface under gravity. The peeling off mode is so effective that all frost departs from the superhydrophobic surface without any droplets residual. When the frosting duration is short and the frost quantity is little, the melting frost jumps off from the superhydrophobic surface. During defrosting for little frost quantity, the volume shrinkage effect dominates, making frost layer break up into many small pieces of frost with irregular shapes. These irregular frost pieces continue to shrink as melting goes, releasing large amounts of surface energy which drive the melting frost to jump off from the superhydrophobic surface. However, as the jumping motion is influenced by many factors and limited by energy transformation, not every frost piece would jump. Therefore, the jumping off mode is not as effective as the peeling off mode that there are still some small droplets adhering on the surface after defrosting. The statistical residual droplet radii in experiments are consistent with the theoretical results. We hope this work could provide guide for real defrosting operation in related engineering fields such as aircrafts, heat exchangers and wind turbines.

Associated content

Supporting information

Video S1 shows the frost peels off from the vertical superhydrophobic surfaces during defrosting when the frosting time is 20 min; Video S2 shows the frost peels off from the vertical superhydrophobic surfaces during defrosting when the frosting time is 30 min; Video S3 shows the frost jumps off from the vertical superhydrophobic surfaces during defrosting when the frosting time is 10 min.

Author information

Corresponding author
*E-mail: wuxiaomin@mail.tsinghua.edu.cn. Tel: +86-10-62770558.
ORCID
Fuqiang Chu: 0000-0002-4054-143X
Dongsheng Wen: 0000-0003-3492-7982
Xiaomin Wu: 0000-0001-7703-0038

Notes

The authors declare no competing financial interest.

Acknowledgements

This work was supported by the Supporting Program for Postdoctoral Innovative Talents of China (No.BX20180024), the National Natural Science Foundation of China (No.51476084) and the 111 Project of China (No.B18002).

References

1. Lynch, F. T.; Khodadoust, A., Effects of ice accretions on aircraft aerodynamics. Progress in Aerospace Sciences 2001, 37, 669-767.
2. Rafati Nasr, M.; Fauchoux, M.; Besant, R. W.; Simonson, C. J., A review of frosting in air-to-air energy exchangers. Renewable and Sustainable Energy Reviews 2014, 30, 538-554.
3. Parent, O.; Ilinca, A., Anti-icing and de-icing techniques for wind turbines: Critical review. Cold Regions Science and Technology 2011, 65 (1), 88-96.
4. Cao, L.; Jones, A. K.; Sikka, V. K.; Wu, J.; Gao, D., Anti-icing superhydrophobic coatings. Langmuir 2009, 25 (21), 12444-8.
5. Huang, L.; Liu, Z.; Liu, Y.; Gou, Y., Preparation and anti-frosting performance of super-hydrophobic surface based on copper foil. Int. J. Therm. Sci. 2011, 50 (4), 432-439.
6. Zhao, Y.; Yang, C., Retarded condensate freezing propagation on superhydrophobic surfaces patterned with micropillars. Applied Physics Letters 2016, 108 (6), 061605.
7. Lv, J.; Song, Y.; Jiang, L.; Wang, J., Bio-inspired strategies for anti-icing. ACS Nano 2014, 8 (4), 3152-69.
8. Schutzius, T. M.; Jung, S.; Maitra, T.; Eberle, P.; Antonini, C.; Stamatopoulos, C.; Poulikakos, D., Physics of icing and rational design of surfaces with extraordinary icephobicity. Langmuir 2015, 31 (17), 4807-21.
9. He, M.; Wang, J.; Li, H.; Song, Y., Super-hydrophobic surfaces to condensed micro-droplets at temperatures below the freezing point retard ice/frost formation. Soft matter 2011, 7 (8), 3993.
10. Jung, S.; Dorrestijn, M.; Raps, D.; Das, A.; Megaridis, C. M.; Poulikakos, D., Are superhydrophobic surfaces best for icephobicity? Langmuir 2011, 27 (6), 3059-66.
11. Guo, P.; Zheng, Y.; Wen, M.; Song, C.; Lin, Y.; Jiang, L., Icephobic/anti-icing properties of micro/nanostructured surfaces. Adv. Mater. 2012, 24 (19), 2642-8.
12. Wen, M.; Wang, L.; Zhang, M.; Jiang, L.; Zheng, Y., Antifogging and icing-delay properties of composite micro- and nanostructured surfaces. ACS Appl. Mater. Interfaces 2014, 6 (6), 3963-8.
13. Boreyko, J. B.; Collier, C. P., Delayed frost growth on jumping-drop superhydrophobic surfaces. ACS Nano 2013, 7 (2), 1618-27.
14. Hao, Q.; Pang, Y.; Zhao, Y.; Zhang, J.; Feng, J.; Yao, S., Mechanism of delayed frost growth on superhydrophobic surfaces with jumping condensates: more than interdrop freezing. Langmuir 2014, 30 (51), 15416-22.
15. Kim, A.; Lee, C.; Kim, H.; Kim, J., Simple approach to superhydrophobic nanostructured Al for practical antifrosting application based on enhanced self-propelled jumping droplets. ACS Appl. Mater. Interfaces 2015, 7 (13), 7206-13.
16. Varanasi, K. K.; Deng, T.; Smith, J. D.; Hsu, M.; Bhate, N., Frost formation and ice adhesion on superhydrophobic surfaces. Applied Physics Letters 2010, 97 (23), 234102.
17. Chu, F.; Wu, X.M.; Wang, L., Meltwater Evolution during Defrosting on Superhydrophobic Surfaces. ACS Appl. Mater. Interfaces 2018, 10 (1), 1415-1421.
18. Boreyko, J. B.; Srijanto, B. R.; Nguyen, T. D.; Vega, C.; Fuentes-Cabrera, M.; Collier, C. P., Dynamic defrosting on nanostructured superhydrophobic surfaces. Langmuir 2013, 29 (30), 9516-24.
19. Chen, X.; Ma, R.; Zhou, H.; Zhou, X.; Che, L.; Yao, S.; Wang, Z., Activating the microscale edge effect in a hierarchical surface for frosting suppression and defrosting promotion. Scientific Reports 2013, 3, 2515.
20. Boreyko, J.; Chen, C.-H., Self-Propelled Dropwise Condensate on Superhydrophobic Surfaces. Phys. Rev. Lett. 2009, 103 (18),

184501.

21. Chu, F.; Wu, X.M.; Zhu, B.; Zhang, X., Self-propelled droplet behavior during condensation on superhydrophobic surfaces. Applied Physics Letters 2016, 108 (19), 194103.
22. Chu, F.; Wu, X.M.; Wang, L., Dynamic melting of freezing droplets on ultraslippery superhydrophobic surfaces. ACS Appl. Mater. Interfaces 2017, 9, 8420-8425.
23. Liu, X.; Chen, H.; Zhao, Z.; Wang, Y.; Liu, H.; Zhang, D., Self-jumping Mechanism of Melting Frost on Superhydrophobic Surfaces. Scientific Reports 2017, 7 (1).
24. Li, D.; Qian, C.; Gao, S.; Zhao, X.; Zhou, Y., Self-propelled drop jumping during defrosting and drainage characteristic of frost melt water from inclined superhydrophobic surface. International Journal of Refrigeration 2017, 79, 25-38.
25. Jing, T.; Kim, Y.; Lee, S.; Kim, D.; Kim, J.; Hwang, W., Frosting and defrosting on rigid superhydrohobic surface. Appl. Surf. Sci. 2013, 276, 37-42.
26. Wang, F.; Liang, C.; Zhang, X., Visualization study of the effect of surface contact angle on frost melting process under different frosting conditions. International Journal of Refrigeration 2016, 64, 143-151.
27. Liu, Y.; Kulacki, F. A., An experimental study of defrost on treated surfaces: Effect of frost slumping. Int. J. Heat Mass Transfer 2018, 119, 880-890.
28. Liang, C.; Wang, F.; Lü, Y.; Yang, M.; Zhang, X., Experimental and theoretical study of frost melting water retention on fin surfaces with different surface characteristics. Exp. Therm. Fluid Sci. 2016, 71, 70-76.
29. Murphy, K. R.; McClintic, W. T.; Lester, K. C.; Collier, C. P.; Boreyko, J. B., Dynamic Defrosting on Scalable Superhydrophobic Surfaces. ACS Appl. Mater. Interfaces 2017, 9 (28), 24308-24317.
30. Kim, H.; Jin, G.; Jeon, J.; Lee, K.-S.; rip Kim, D., Defrosting behavior and performance on vertical plate for surfaces of varying wettability. Int. J. Heat Mass Transfer 2018, 120, 481-489.
31. Chu, F.; Wu, X.M., Fabrication and condensation characteristics of metallic superhydrophobic surface with hierarchical micro-nano structures. Appl. Surf. Sci. 2016, 371, 322-328.
32. Chu, F.; Wu, X.M.; Ma, Q., Condensed droplet growth on surfaces with various wettability. Applied Thermal Engineering 2017, 115, 1101-1108.
33. Zhang, X.; Wu, X.M.; Min, J., Freezing and melting of a sessile water droplet on a horizontal cold plate. Exp. Therm. Fluid Sci. 2017, 88, 1-7.
34. Wang, F.-C.; Yang, F.; Zhao, Y.-P., Size effect on the coalescence-induced self-propelled droplet. Applied Physics Letters 2011, 98 (5), 053112.
35. Enright, R.; Miljkovic, N.; Sprittles, J.; Nolan, K.; Mitchell, R.; Wang, E. N., How Coalescing Droplets Jump. ACS Nano 2014, 8 (10), 10352-10362.
36. Kim, M. K.; Cha, H.; Birbarah, P.; Chavan, S.; Zhong, C.; Xu, Y.; Miljkovic, N., Enhanced Jumping-Droplet Departure. Langmuir 2015, 31 (49), 13452-66.
37. Santos, M. J.; Velasco, S.; White, J. A., Simulation analysis of contact angles and retention forces of liquid drops on inclined surfaces. Langmuir 2012, 28 (32), 11819-26.
38. Gao, N.; Geyer, F.; Pilat, D. W.; Wooh, S.; Vollmer, D.; Butt, H.-J.; Berger, R., How drops start sliding over solid surfaces. Nature Physics 2017, 14 (2), 191-196.
39. Bommer, S.; Scholl, H.; Seemann, R.; Kanhaiya, K.; Sheraton, V. M.; Verma, N., Depinning of drops on inclined smooth and topographic surfaces: experimental and lattice Boltzmann model study. Langmuir 2014, 30 (37), 11086-95.
40. ElSherbini, A. I.; Jacobi, A. M., Liquid drops on vertical and inclined surfaces; I. An experimental study of drop geometry. J Colloid Interface Sci. 2004, 273 (2), 556-65.

Table of contents